Binding between Proteins and Cationic Spherical Polyelectrolyte Brushes: Effect of pH, Ionic Strength, and Stoichiometry

ARTICLE *in* BIOMACROMOLECULES · FEBRUARY 2013

Impact Factor: 5.75 · DOI: 10.1021/bm301865g · Source: PubMed

4 AUTHORS, INCLUDING:

Kaimin Chen
Shanghai Jiao Tong University
23 PUBLICATIONS **254** CITATIONS
SEE PROFILE

Li Li
University of Science and Technology of China
104 PUBLICATIONS **571** CITATIONS
SEE PROFILE

Article

pubs.acs.org/Biomac

Binding between Proteins and Cationic Spherical Polyelectrolyte Brushes: Effect of pH, Ionic Strength, and Stoichiometry

Siyi Wang,[†,§] Kaimin Chen,[†,‡,§] Li Li,*[,†] and Xuhong Guo*[,†]

[†]State Key Laboratory of Chemical Engineering, East China University of Science and Technology, Shanghai 200237, People's Republic of China

[‡]Med-X Research Institute, Shanghai Jiao Tong University, Shanghai 200030, People's Republic of China

ABSTRACT: Cationic spherical polyelectrolyte brushes (SPBs) were synthesized by photoemulsion polymerization, consisting of a polystyrene core with a diameter around 80 nm and a poly(2-aminoethylmethacrylate hydrochloride) (PAEMH) shell with a thickness from 10 to 50 nm densely grafted on the core surface. The binding of various proteins onto SPBs was observed by turbidimetric titration, dynamic light scattering (DLS), zeta potential, and isothermal titration calorimetry (ITC). The binding, aggregation, and releasing of proteins by SPB can be tuned by modulating pH. The pH regions of binding for bovine serum albumin (BSA), β-lactoglobulin (BLG), and papain onto SPBs are markedly different and tunable by ionic strength and stoichiometry between protein and SPB. Binding energetics, affinity, and amount of various proteins onto cationic SPBs were determined by ITC. These findings lay the foundation for SPB applications in the protein purification and selective immobilization of different proteins, enzymes, and antibodies.

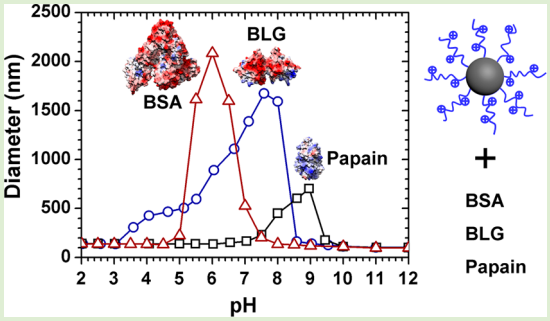

1. INTRODUCTION

In recent years, the interaction between protein and polyelectrolyte has attracted many interests in glycobiology, tissue engineering, biosensing, and pharmacology, which has led to multiple applications in protein separation, drug delivery, and wound repair.[1−3] Nanoparticles can be easily modified with other functional molecules to realize various nanobiotechnological separations and detections.[4,5] Since they are small enough to interact with cellular machinery and potentially to reach previously inaccessible targets, such as the brain, nanoparticles can be used as carriers for proteins, DNA, enzymes, and antibodies.[6] Spherical polyelectrolyte brushes (SPBs) are very suitable for the immobilization of biomacromolecules in aqueous solution without biofouling and reduction in biological activity.[7−9] Because SPBs can modulate and keep ionic strength and pH stable in a certain range within the shell layers due to the Donnan effect,[10−13] they can serve as a buffer-like shelter for proteins and enzymes in aqueous solutions. Driven by electrostatic attraction and hydrophobic interactions,[9,14−16] SPBs are capable of adsorbing and binding with many proteins. Additionally, bound proteins by SPBs can be released through changing the ionic strength of the system.[8] SPBs with magnetic nanoparticles in the core become recyclable after the immobilization of proteins.[17−19] Therefore, SPBs should be ideal candidates for protein immobilization, drug delivery, protein separation,[17,18] high-performance diagnostic assay, and nanoreactors.[3,19−21]

Anionic spherical polyelectrolyte brushes have been proven to be suitable for the immobilization of proteins and enzymes by Ballauff and co-workers.[7−9,22,23] It seems that cationic SPBs provide stronger binding affinity and larger binding amount for acidic proteins according to Dubin and co-workers, who have studied the complexation and aggregation between proteins and linear cationic polyelectrolytes in aqueous solution.[24−28] Because the majority of proteins are acidic proteins with net negative charge, the electrostatic attraction between acidic proteins and cationic SPBs should be enhanced. To the best of our knowledge, until now, no experiments on the selective binding of various proteins by cationic SPBs in the full range of pH have been reported. The only report concerning the adsorption of proteins to cationic SPBs was by Ballauff et al., who used isothermal titration calorimetry (ITC) to observe the adsorption isotherm of bovine pancreatic ribonuclease A (RNase A) on cationic SPBs as a function of temperature and ionic strength at physiological pH 7.2.[29] However, most papers involved only a single protein,[9,22,29,30] while proteins with different isoelectric points, molecular weights, or shapes must influence their adsorption onto nanoparticles.[31] Furthermore, almost no paper on polyelectrolyte−protein interactions focused on the various phase behaviors concerning adsorption, aggregation, and releasing.

In this paper, the cationic SPBs were synthesized by photoemulsion polymerization, and employed to bind bovine serum albumin (BSA), β-lactoglobulin (BLG), and papain, respectively (Scheme 1). The effect of pH on binding for various proteins onto cationic SPBs was observed by

Received: December 5, 2012
Revised: January 28, 2013
Published: February 13, 2013

dx.doi.org/10.1021/bm301865g | Biomacromolecules 2013, 14, 818−827

Scheme 1. Schematic Representation of the Synthesis of Annealed Cationic SPBs and the Consequent Binding of Proteins[a]

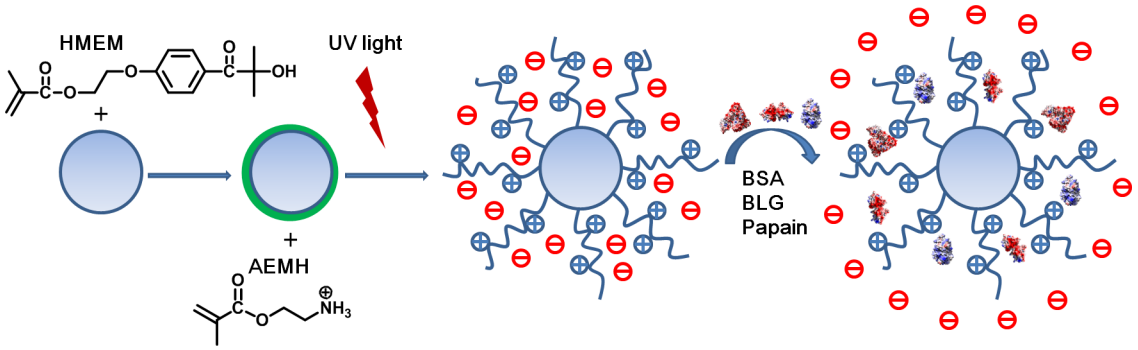

[a]The HMEM is a home-made photoinitiator (2-[p-(2-hydroxy-2-methylpropiophenone)]-ethyleneglycol-methacrylate), and AEMH is the cationic monomer 2-aminoethylmethacrylate hydrochloride.

turbidimetric titration, dynamic light scattering (DLS) and zeta potential. ITC was employed to determine the amount, affinity, and thermodynamics of proteins binding onto SPBs. The binding stoichiometry, architecture, and phase state of the complex between protein and SPB were modulated by changing pH, ionic strength, and bulk stoichiometry. This work can lay the foundation for protein purification and separation by SPBs under optimal conditions.

2. EXPERIMENTAL SECTION

2.1. Materials. BLG, papain, 2-aminoethylmethacrylate hydrochloride (AEMH), and standard sodium hydroxide (NaOH) solution (0.1 M) were purchased from Sigma-Aldrich and used without further purification. Styrene was distilled under reduced pressure and stored in a refrigerator at 4 °C before use. BSA, sodium chloride (NaCl), hydrochloric acid (HCl), standard phosphate solutions, cetyltrimethylammonium bromide (CTAB), 2,2′-azobis(2-methylpropionamidine) dihydrochloride (AIBA), and 2-(*N*-morpholino) ethanesulfonic acid (MES) were purchased from J & K Chemical and used as received. All water used in this work was purified by reverse osmosis and subsequent ion exchange (Millipore Milli-Q). 2-Hydroxy-4′-hydroxyethoxy-2-methylpropiophenone (IRGACURE 2959, Ciba), and methacryloyl chloride purchased from TCI were used without purification.

2.2. Synthesis of Cationic Spherical Polyelectrolyte Brushes. Cationic SPBs with polystyrene (PS) core and poly(2-aminoethylmethacrylate hydrochloride) (PAEMH) brush[32−34] were synthesized by photoemulsion polymerization.[10,35] The obtained cationic SPBs consisted of a PS core (78 ± 2 nm) and a PAEMH brush layer with the thickness of 13 to 54 ± 5 nm. The doses of monomer AEMH were 25%, 50%, and 75% (molar percent of the amount of styrene for core), respectively. The synthesis of spherical PAEMH brushes is divided into three steps (Scheme 1): In the first step, narrowly distributed PS core latex was prepared by conventional emulsion polymerization.[10,35] In the second step, a thin shell of the homemade photoinitiator (2-[p-(2-hydroxy-2-methylpropiophenone)]-ethyleneglycol-methacrylate) (HMEM) prepared by a Schotten−Baumann reaction[35] was generated on the core under slow addition of HMEM to ensure a well-defined photoinitiator layer on the core surface.[10,35] In the final step, AEMH monomer was added, and the entire system was illuminated by UV−visible (UV−Vis) radiation in a photoreactor with constant stirring by a magnetic stirrer in 30 min. Radicals will thus be generated by photoinitiation on the surface of the nanoparticles and start the radical polymerization of the monomer.[10,35,36] Spherical PAEMH brushes thus grew on the PS core surface (Scheme 1).

2.3. Determination of SPB Grafting Density. To determine the grafting density, SPB chains were cut off from the core surface. The cleaving process of PAEMH chains from SPBs (50 mol %) was under strong base (2 M NaOH) conditions after 10 days at 120 °C. After cleaving off the chains from the core particles, the molecular weight and molecular weight distribution were determined by gel permeation chromatography (GPC, 2414 refractive index detector, Waters) using poly(2-vinylpyridine) (P2VP) as the standards and 0.3 M NaCl plus 5% (w/v) acetic acid as the eluent. The number average molecular weight M_n of cleaved chains was 25 900 g/mol with a polydispersity index (PDI) of 1.68. This PDI value is typical for a free radical polymerization. The contour length of the chains was 39 nm determined using M_n from the GPC measurements. Considering the mass ratio and M_w of the polyelectrolyte chains, we calculated a grafting density of 0.06 chains nm^{-2}. Using the mass ratio we also calculated the number of charged units per SPB particle of 1146.

2.4. Adsorption Experiments. The ionic strength of all aqueous solutions of SPBs (5 mg/mL) in MES buffer was tuned through the addition of NaCl. The pH of solutions was adjusted with NaOH or HCl standard aqueous solutions. BSA solutions were prepared by adding BSA into MES buffer solutions. After mixing of BSA and SPBs, the immobilization of protein by SPBs was stirred for 24 h at 4 °C for equilibration. All samples were centrifuged (Microfuge 16, Centrifuge, Brinkmann) with 10000 rpm for 60 min at room temperature. Also, the supernatants were filtered by a 0.20 μm RC membrane (Corning Incorporated). The amount of unbound proteins was determined spectroscopically from the supernatant at 280 nm (UV-2550, UV−Vis spectrophotometer, SHIMADZU). The amount of immobilized proteins was calculated by subtracting the amount of unbound proteins from the total amount of proteins.[8,9,38,39]

2.5. Turbidimetric and pH Titration. Transmittance (%T) was monitored with a Brinkmann PC 950 colorimeter (420 nm filter), connected to a 2 cm path length optical probe. The turbidity was reported as 100-%T, and the fluctuations (±0.1%) of transmittance were treated by consistently selecting the highest transmittance. All solutions were prepared with water and filtered through 0.45 μm filters. The dependence of solution turbidity on pH was obtained by observing the change of turbidity upon addition of 0.1 M NaOH and/or 0.1 M HCl to a protein−SPB mixture at a constant ionic strength. Generally, SPB and protein concentrations were 0.004 and 0.020 g/L, respectively. A 2.0 mL microburet was used to add standard NaOH or HCl solutions to a 100 mL aqueous solution of SPBs adjusted to the desired ionic strength by NaCl. A nitrogen purge was employed during all titrations. SPB-free blanks and protein-free blanks were subtracted to eliminate the effect of free protein scattering. An Orion pH meter (Ross Ultra Combination pH, 8156BNUWP, Orion) was used to monitor the solution pH.

2.6. Dynamic Light Scattering and Zeta Potential. The diameters of SPB and zeta potentials of protein−SPB complexes were determined by DLS (Zeta Potential/Particle Sizer NICOMP 380 ZLS instrument) at variable pH at 25 °C and at a scattering angle of 90°. Size of protein−SPB complexes was tested in 1 mM NaCl solution. Protein and SPB concentrations were 0.040 and 0.008 mg/mL for DLS, respectively. In the zeta potential measurement, the electronic field was 5 V/cm in constant-current mode. Zeta potential of complexes was measured in 1 mM NaCl solution, and the pH of the

dx.doi.org/10.1021/bm301865g | Biomacromolecules 2013, 14, 818−827

sample was adjusted with HCl and NaOH. Protein and SPB concentrations were 0.40 mg/mL and 0.08 mg/mL for zeta potential, respectively. For control experiments, SPB concentration was 0.08 mg/mL and BSA concentration was 10 mg/mL to obtain a high signal-to-noise ratio.

The diameter of the PS core particles was 78 ± 2 nm, which was measured by DLS via NICOMP distribution analysis using the inverse Laplace transform. The diameters of SPB particles with AEMH doses of 25, 50, and 75 mol % at the ionic strength of 0.1 mM were 118, 147, and 186 ± 5 nm, with the PDI of ca. 0.01. The PDI for intra-SPB complexes and inter-SPB complexes were ca. 0.05 and ca. 0.5, respectively. For the DLS measurements, the suspensions were filtered through a 0.45 μm polytetrafluoroethylene (PTFE) filters (25 mm Syringe Filter, PTFE Membrane, Corning Incorporated).

2.7. Isothermal Titration Calorimetry. The thermodynamic quantities of protein binding onto colloidal particles were determined by ITC (MicroCal ITC_{200}, GE Healthcare). Proteins and SPB solutions were made in 5 mM MES and NaOH buffer at various pH conditions. All solutions were filtered by 0.22 μm Millipore filters. After instrument stabilization at 25 °C, 200 μL of 3.2×10^{-6} mM SPB solution was titrated with 20 successive injections of protein solutions (40 μL of 0.41 mM). The interval between injections was 180 s. The solution was stirred at 1000 rpm in the reaction cell during the experiments. Prior to data analysis, heats of dilutions were corrected by subtracting values for SPB-free blank solutions. ITC data analysis typically employs Microcal Origin software, which (1) convers raw calorimetric data (heat evolved or consumed for each titration step, $\delta\Delta H$) to a binding isotherm, and (2) analyzes the binding isotherm to yield binding site number (size), and binding constants from which ΔG and hence ΔS are obtained. All parameters are model-dependent, and we used a one-site binding model to fit the binding isotherms.

3. RESULTS AND DISCUSSION

3.1. Synthesis and Characterization of Cationic SPBs. The thickness of SPB was calculated by subtracting the hydrodynamic radius of the PS core from the SPBs. As shown in Figure 1a, the thickness of the SPBs increased rapidly at the beginning and reached a plateau after approximately 30 min during the photoemulsion polymerization. The thickness of SPBs increased upon increasing the dose of monomer AEMH from 25 to 75 mol % of the PS cores, while the size distribution of these particles kept narrow as determined by DLS. Therefore, the thickness of SPBs can be tunable by changing the monomer amount.

The obtained cationic SPBs (PAEMH-SPBs) with titratable functional groups were very sensitive to pH and ionic strength, which control the swelling and layer thickness of SPBs. As observed in Figure 1b, the thickness of the SPBs increased rapidly with decreasing pH. Diameters of cationic SPBs reached maxima at low pH, and displayed plateaus at pH < 5 where all the amino groups were charged. The repulsive force among the charged PAEMH chains was enhanced with increasing degree of protonation, and thus led to the stretch of the PAEMH chains and increase of brush thickness.

Interestingly, the thickness of cationic SPBs showed a minimum with increasing the salt concentration, which was shown in Figure 1c. There were two regions of salt concentration affected on the thickness of SPB. The first region is at low salt concentration where the electrostatic repulsive force among the chains of SPB dominates. The added salt ions led to a screening of the electrostatic interaction, which resulted in the shrinking of brush layer.[36,37] The second region is at high salt concentration where the brush layer is reswollen at salt concentration above 0.5 M. The "salting-in" of the cationic brush layer is due to the charge reversal of the cationic chains via the specific interactions between polycation and

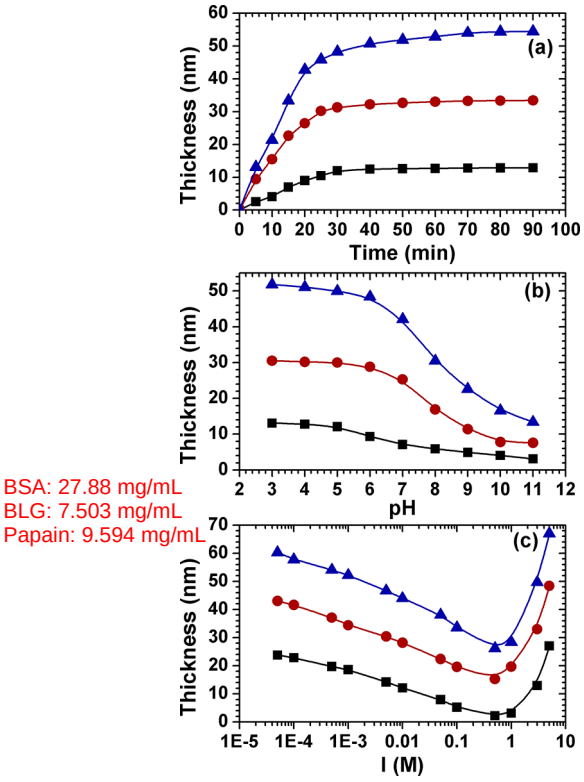

BSA: 27.88 mg/mL
BLG: 7.503 mg/mL
Papain: 9.594 mg/mL

Figure 1. (a) Thickness of PAEMH-SPBs as a function of reaction time determined by DLS during photoemulsion polymerization. (b) Thickness of PAEMH-SPBs as a function of pH in 10 mM NaCl solutions. (c) Thickness of PAEMH-SPBs as a function of salt concentration (NaCl) at pH 5. Symbols denote SPBs with various doses of AEMH monomer: (■) 25 mol %, (●) 50 mol %, and (▲) 75 mol %.

Cl^-.[40] This abnormal phenomenon was also observed by Mei et al.,[37] and they attributed the "salting-in" to the increase of reduced excluded-volume, which is a result of Cl^- adsorption.

3.2. Binding of BSA to Cationic SPBs. BSA is a typical acidic protein that has been mostly studied as a model protein, and here it was also used as a model to investigate the binding event between proteins and cationic SPBs. As shown in Figure 2a, the turbidity of the mixture of BSA and cationic SPBs showed a maximum at pH between 5 and 7. When pH was below 5 or over 7, the turbidity was close to zero. The maximum turbidity increased upon increasing concentration of BSA and SPB with the same bulk stoichiometry.

Turbidity increased slightly from pH 3 to 5, which was attributed to the initial binding of BSA onto SPB and formed intra-SPB complexes. The abrupt increase in turbidity at pH 5 should be due to the formation of aggregation among SPB induced by inter-SPB complexes. At pH range of 6−7, turbidity decreased sharply, which was due to the aggregate dissolution of SPBs. The maximum turbidity can be understood from the maximum aggregate size as indicated in Figure 2b. At higher concentration, more SPB aggregates were formed induced by BSA binding.

It was clear from the data in Figure 2b that the size change of BSA−SPB complexes versus pH was accordant to the variation in turbidity because the turbidity was sensitive to particle size. At low pH, the initial binding of BSA onto SPB may arise from the attraction between positive SPB and negative BSA "charge patch"[26,41−43] or "charge regulation",[44−48] which essentially is a

dx.doi.org/10.1021/bm301865g | Biomacromolecules 2013, 14, 818−827

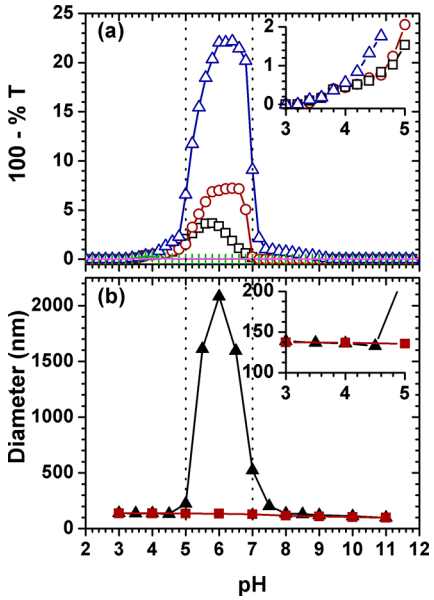

Figure 2. (a) Turbidimetric titration for BSA−SPB as a function of pH at ionic strength of 1 mM with various concentrations. Symbols denote (△) BSA and SPB (with 50 mol % dose of AEMH) concentrations of 0.020 and 0.004 mg/mL, (○) BSA and SPB concentrations of 0.008 and 0.0016 mg/mL, (□) BSA and SPB concentrations of 0.004 and 0.0008 mg/mL, (+) pure BSA, and (---) blank SPB. Bulk stoichiometry was set as 5 for BSA/SPB (w/w). (b) Size of BSA−SPB complexes and free cationic SPB as a function of pH in 1 mM NaCl solutions. BSA and SPB concentrations were 0.040 and 0.008 mg/mL for DLS, respectively. Symbols denote (▲) BSA−SPB complexes and (■) blank cationic SPBs.

protein pK_a shift induced by the electric field of SPBs. With increasing pH above the isoelectric point (pI = 4.9), the negative patches on BSA increased, which led to the stronger binding via electrostatic attraction. Since the particle size of blank SPBs was changed in the range of 40 nm upon increasing pH, the significant increase in turbidity and complex size should be due to the aggregation among SPBs induced by BSA binding. The adsorption of BSA on SPBs reduced the net charge of SPBs and affected the stability, which led to the aggregation among SPBs.

As shown in Figure 3, the decrease in zeta potential upon addition of BSA in SPBs below pH 6 implied that the binding of BSA onto SPBs was probably dominated by electrostatic interaction between acidic proteins and cationic SPBs. The reduction of complex zeta potential was attributed to the bound BSA in SPBs below pH 5.5. The net charge of SPB was partly neutralized by bound BSA.[46,49] At pH around 6, the complex zeta potential was close to zero leading to the aggregation,[25,26,28] which is accordant with the observation by DLS and turbidimetric titration. At pH range from 6 to 7, the complex zeta potential increased again, while both turbidity and complex size showed maxima. This implied that the aggregate dissolution of SPBs and the releasing of BSA from SPBs occurred. When pH was greater than 7, the complex zeta potential coincided with that of the blank SPBs. So the majority of BSA was released from SPBs due to low surface charge of SPBs and excess BSA charge at high pH. The collapse of SPBs with low degree of protonation led to the extrusion of BSA from SPB layers.

The observation of turbidity, complex size, and zeta potential revealed the existence of three interaction domains based on

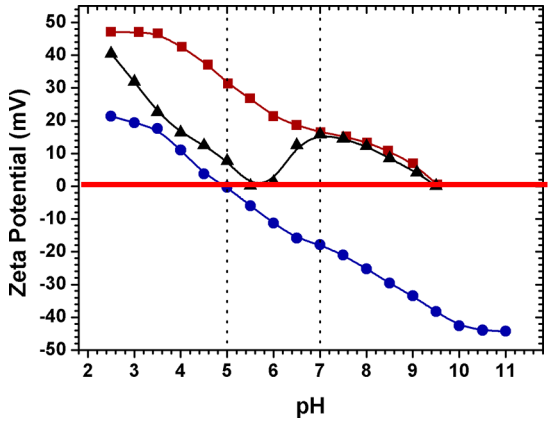

Figure 3. Zeta potential of BSA−SPB complexes, blank cationic SPBs (with 50 mol % dose of AEMH), and blank BSA as a function of pH in 1 mM NaCl solutions. Symbols denote (▲) BSA−SPB complexes, (■) blank cationic SPBs, and (●) blank BSA. Concentrations of BSA and SPBs were 0.40 and 0.08 mg/mL for zeta potential, respectively. Bulk stoichiometry was set as 5 for BSA/SPB (w/w). For the blank sample, BSA concentration was 10 mg/mL to obtain a high signal-to-noise ratio.

pH: (1) dynamic equilibrium binding of BSA in SPB to form intra-SPB complexes (binding at low pH), (2) kinetic aggregation of SPBs induced by BSA binding to form inter-SPB complexes (aggregation at moderate pH), and (3) dynamic equilibrium releasing of BSA from SPBs (releasing at high pH) (Scheme 2). Furthermore, the two critical pHs between neighboring domains were independent of concentrations of BSA and cationic SPB.

Scheme 2. Schematic Representation of the Binding between Protein and SPBs in Different pH Regions

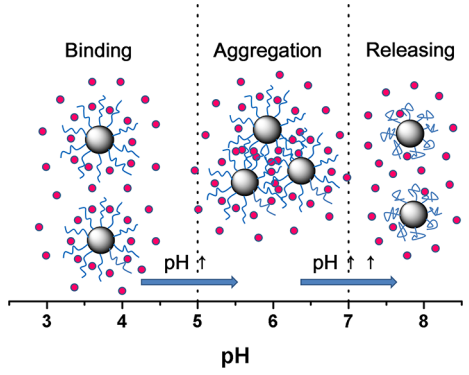

To further illustrate the binding event between cationic SPBs and BSA, ITC was applied to determine the thermodynamic parameters under critical conditions. An ideal isothermal curve was obtained from ITC at pH 7.1, corresponding to the point between the aggregation and releasing regions. The ITC data for SPBs with BSA is shown in Figure 4. The vertical peaks correspond to the heat change in the sample cell containing SPBs at each protein injection. The binding heat is negative, indicating that the complexation[50] between BSA and SPBs is exothermic, which corresponds to a dominated electrostatic attraction between the oppositely charged surfaces. The driving force for the protein adsorption is, therefore, of enthalpic origin.[29,31,51−54]

dx.doi.org/10.1021/bm301865g | *Biomacromolecules* 2013, 14, 818−827

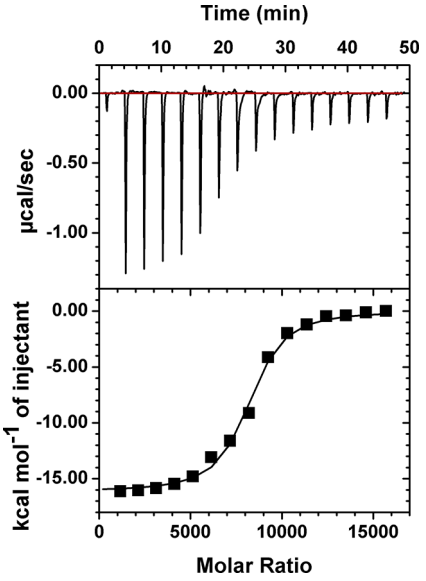

Figure 4. Isothermal titration calorimetry (ITC) data for the binding of BSA onto SPB (with 75 mol % dose of AEMH) in MES buffer at pH 7.1 and ionic strength of 5 mM. The upper panel shows the raw data of the ITC. The integrated heats of each injection (solid square) and one-site binding fitting (solid line) are shown in the lower panel. A 200 μL aliquot of 3.2 × 10^{-6} mM SPB solution was titrated with injections of BSA solutions (40 μL of 0.41 mM).

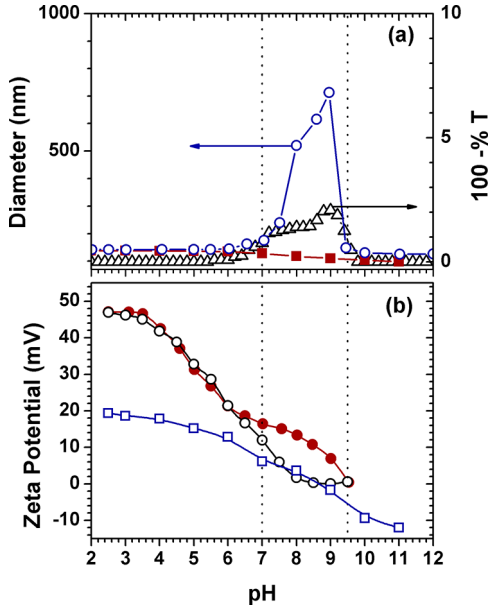

Figure 5. (a) Size and turbidity for the papain−SPB complex as a function of pH in 1 mM NaCl. Symbols denote (○) size of papain−SPB, (■) size of blank SPBs (with 50 mol % dose of AEMH), and (△) turbidity for papain−SPB. Concentrations of papain and SPBs are 0.020 and 0.004 mg/mL for turbidimetric titration, and 0.040 and 0.008 mg/mL for DLS, respectively. Bulk stoichiometry was 5 for papain/SPB (w/w). (b) Zeta potential of papain−SPB as a function of pH in 1 mM NaCl. Symbols denote (○) papain−SPB, (●) blank SPBs, and (□) blank papain. Papain and SPB concentrations were 0.40 and 0.08 mg/mL for zeta potential, respectively. Blank papain concentration was 10 mg/mL to obtain a high signal-to-noise ratio.

In order to figure out the selectivity of cationic SPBs to different proteins, two other proteins with opposite charge, papain, and similar pI, BLG, were applied to investigate their binding region, affinity, and stoichiometry to cationic SPBs.

3.3. Binding of Papain and BLG. In Figure 5a, both turbidity and size of papain−SPB complexes displayed maxima at pH 9, which were observed by turbidimetric titration and DLS. The initial binding of papain onto SPBs and the formation of intra-SPB complexes led to the slight increase in turbidity and size in the pH range from 6 to 7. The aggregation among SPBs induced by papain binding and the formation of inter-SPB complexes contributed to the obvious increase in turbidity and size in the pH range from 7 to 9. Upon the increasing pH from 9 to 9.5, the decreasing turbidity and size were due to the aggregate dissolution of SPBs. The zeta potential shown in Figure 5b was also consistent with the turbidity and DLS results: the zeta potential of papain−SPB complexes decreased with increasing pH. Complex zeta potential was lower than that of blank SPBs in the pH range from 6 to 9 and coincided with that of the blank SPBs at pH 9.5.

Figure 5 revealed that the binding of papain onto cationic SPBs also included the three domains, which was similar to that of BSA (Scheme 2). However, the pH regions of binding, aggregation, and releasing of papain by SPBs were significantly different from that of BSA (as shown in Table 1). Compared to BSA, the onset of binding for papain onto SPBs was shifted to higher pH, and the pH region of binding was narrowed. At acidic pH far from the isoelectric point of papain (pI = 8.8), papain has no effective negative charge patches to bind with SPBs at pH < 6.

Furthermore, the complex turbidity and aggregation size are much smaller than those of BSA, which probably reflected the weaker binding between papain and SPBs. These differences between papain and BSA binding onto SPBs arose from their different properties (pI, molecular weight, and hydrodynamic size), which are summarized in Table 2 and illustrated in Scheme 3. Acidic proteins have much more negative charges than basic proteins at the same pH. So, based on electrostatics, the interaction between acidic protein (BSA) and cationic SPBs should be much stronger in a wide pH range than basic protein (papain), and the higher binding affinity and stoichiometry (see discussion in the following) may come from a larger charge patch.

Table 1. pH Regions of Binding Event for Various Proteins to Cationic SPBs

	binding	aggregation	releasing
BSA-SPB	pH 3.0−5.0	pH 5.0−7.0	pH > 7.0
BLG-SPB	pH 2.5−3.5	pH 3.5−8.5	pH > 8.5
Papain-SPB	pH 6.0−7.0	pH 7.0−9.5	pH > 9.5

Table 2. Properties of Various Proteins

protein	pI	MW	diameter (nm)[a]
BSA	4.9	68 000	7.2 ± 0.2
BLG[b]	5.1	36 600	4.8 ± 0.1
papain	8.8	23 400	4.6 ± 0.1

[a]Diameters of proteins were measured by a Malvern Nano ZS instrument. The protein concentration was set as 1 mg/mL, and each protein was dissolved in a 5 mM phosphate buffer. [b]The diameter of BLG at measured conditions indicated a dimer, and the MW here is also for a dimer.

dx.doi.org/10.1021/bm301865g | Biomacromolecules 2013, 14, 818−827

Scheme 3. Columbic Surface Contours (−10 (red) and +10 kcal/mol·*e* (blue)) for BSA (left, PDI ID: 3V03), BLG (middle, PDI ID: 1BEB), and Papain (right, PDI ID: 9PAP) at pH 7 without Addition of Salt[a]

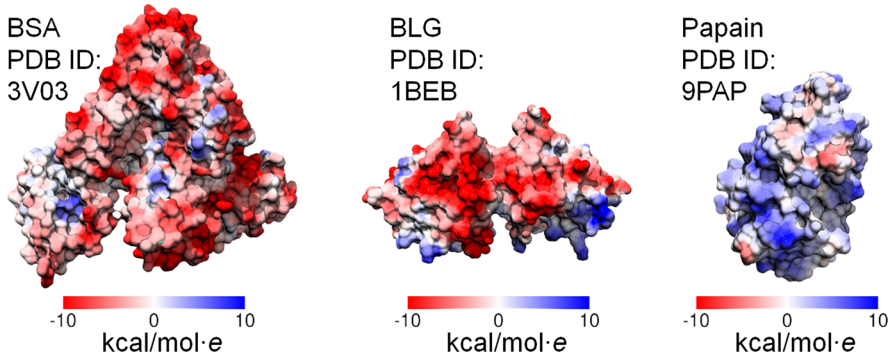

[a]Produced by using the Chimera 1.6.1 program.

Not only the isoelectric point, but protein molecular weight, shape, and charge anisotropy also influence binding onto SPBs. Figure 6 signified the similar transition upon changing pH for BLG−SPB to BSA−SPB, which was observed by combining turbidimetric titration, DLS, and zeta potential. Features of the BLG−SPB system at 2 < pH < 12 in Figure 6 were described in terms of the formation of intra-SPB complexes (2.5 < pH < 3.5), inter-SPB complexes (3.5 < pH < 8.5), and releasing of BLG from SPBs (pH > 8.5).

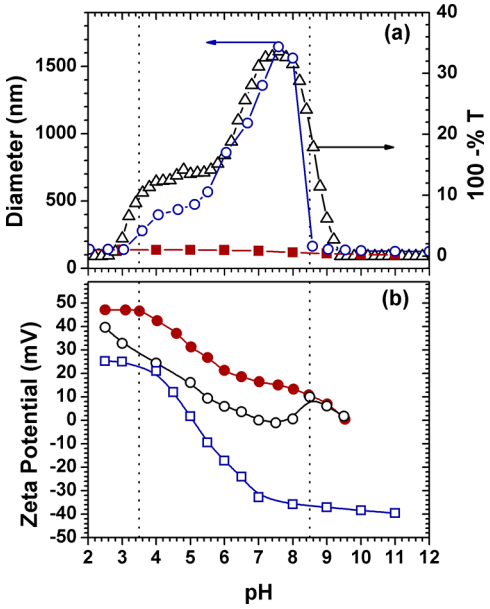

Figure 6. Size and turbidity for BLG−SPB complex as a function of pH in 1 mM NaCl. Symbols denote (○) size of BLG−SPB, (■) size of blank SPBs (with 50 mol % dose of AEMH), and (△) turbidity for BLG−SPB. Concentrations of BLG and SPBs are 0.020 and 0.004 mg/mL for turbidimetric titration, and 0.040 and 0.008 mg/mL for DLS, respectively. Bulk stoichiometry was 5 for BLG/SPB (w/w). (b) Zeta potential of BLG−SPB as a function of pH in 1 mM NaCl. Symbols denote (○) BLG−SPB, (●) blank SPBs, and (□) blank BLG. BLG and SPB concentrations were 0.40 and 0.08 mg/mL for zeta potential, respectively. Blank BLG concentration was 10 mg/mL to obtain a high signal-to-noise ratio.

Compared to BSA, BLG exhibited a wider pH region of binding and higher complex turbidity relative to the binding amount. Both BSA and BLG are acidic proteins with similar pI, but these two proteins are different in "charge patch"[26,41−43] or "charge regulation".[44−48] BLG has a larger negative charge patch than BSA, which can be demonstrated by the simulation with DelPhi.[26,42,43,52,53] Negative charge patch of BLG appeared at a low pH, which contributed to the earlier binding with pH. And the larger negative charge patch delayed the releasing of BLG from SPBs to a high pH.

The complex turbidity and size curves were very different between BSA−SPB and BLG−SPB binding. The BLG−SPB complexes displayed a plateau in the pH range from 4 to 6, which may result from BLG charge anisotropy. When pH is near 3.5, the negative charge patch of BLG becomes obvious and leaves the positive charge patch of BLG on the small aggregates outward.[53] Outside, the positive charge patch maintained in the pH range referred to the plateau, and diminished at pH beyond the plateau resulting in further aggregation. The absence of plateau for BSA−SPB binding was attributed to the discrete charge distribution on BSA.[53]

We have used qualitative methods to compare the different architectures and phase states among various proteins binding onto SPBs. In the following, the different binding stoichiometries among various proteins were investigated by ITC quantitatively. Figures 7 and 8 show the binding affinity and binding stoichiometry of papain and BLG onto SPBs by ITC. The signal that was observed for the binding of papain and BLG onto SPBs was exothermic throughout the entire range. This finding immediately indicated that the driving force for papain and BLG binding may be enthalpic origin. The molar ratio of bound papain and BLG onto SPBs can be obtained by one-site binding fitting of the integrated binding heat in Figures 7 and 8.

Binding between SPBs and proteins occurs if the total free energy of the system is reduced. The enthalpic contribution to the binding of proteins onto SPBs was positive, while entropic contribution for BSA and BLG was negative, and for papain was positive (Table 3). The positive effect of entropy gain on protein binding was due to the release of counterions and water molecules during the process, while the aggregation of SPBs induced by protein binding and association among protein dimers in the adsorbed state should be followed by a negative entropic effect. So the entropic effect was positive when entropic gain originated from protein binding onto SPBs was larger than that originated from the aggregation and association.

Binding stoichiometry depends on both binding constant and protein size. As can be seen from Table 3, the binding

dx.doi.org/10.1021/bm301865g | *Biomacromolecules* 2013, 14, 818−827

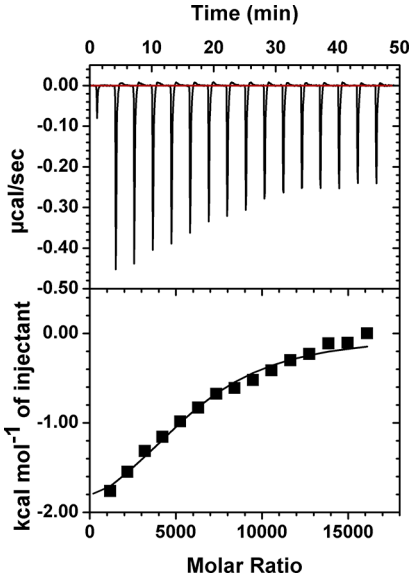

Figure 7. ITC data for the binding of papain onto SPB (with 75 mol % dose of AEMH) in MES buffer at pH 9.5 and ionic strength of 5 mM. The upper panel shows the raw data of the ITC. The integrated heats of each injection are shown in the lower panel together with the fit of the one-site binding model. A 200 μL of 3.2×10^{-6} mM SPB solution was titrated with injections of papain solutions (40 μL of 0.41 mM).

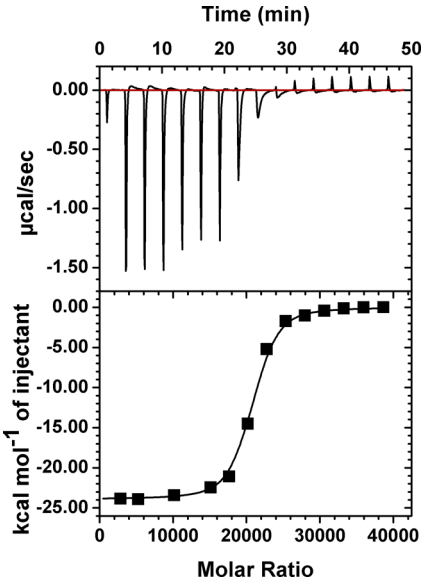

Figure 8. ITC data for the binding of BLG onto SPBs (with 75 mol % dose of AEMH) in MES buffer at pH 8.8 and ionic strength of 5 mM. The upper panel shows the raw data of the ITC. The integrated heats of each injection are shown in the lower panel together with the fit of the one-site binding model. A 200 μL of 3.2×10^{-6} mM SPB solution was titrated with injections of BLG solutions (40 μL of 0.41 mM).

constant (K_{obs}) of BSA−SPB was approximately 15 times greater than that of papain, while it was approximately 7 times smaller than that of BLG. Also, the binding stoichiometries (N) of BLG, BSA, and papain onto SPBs are 19000, 7900, and 5700, respectively. Although the size of papain is very close to that of BLG, papain−SPB has a lower binding stoichiometry due to a low binding constant compared to BLG−SPB. Stoichiometry of BLG−SPB is more than two times compared to BSA−SPB, while size of BSA is only 1.5 fold of BLG, which should be due to a large binding constant for BLG−SPB. The large binding constant of BLG−SPB compared to BSA−SPB resulted from the larger negative charge patch for BLG.

3.4. Effect of Ionic Strength and Bulk Stoichiometry.

We have discussed the effect of pH on the binding of proteins onto SPB above. The binding of proteins onto SPB is reversible with pH. While the swelling and charge density of cationic SPB are controlled not just by pH, but also by ionic strength. On the other hand, proteins are effectively released from SPB due to the significant loss of attractive force in high salt concentration solution. Ionic strength also influences the presentation of protein "charge patches"[26,41−43] or "charge regulation"[44−48] to SPB. If protein concentration changed, the total amount of charges would change in the system. So the bulk stoichiometry and initial concentration in the mixed solution may also affect the binding region of proteins onto SPB. In the following, we discussed the effects of ionic strength and bulk stoichiometry on the binding of proteins onto SPB, using BSA as the model protein.

Figure 9a shows the binding amount of BSA per unit weight of SPBs (τ_{ads}) as a function of the concentration of original protein in solution (C_p) at different ionic strength determined by UV−Vis spectroscopy. The binding amount of BSA by SPBs decreased monotonically upon increasing the ionic strength from 1 to 1000 mM, and displayed a plateau at high protein concentration where the adsorption reached saturation.[8,9,38,39]

Figure 9b shows the effect of ionic strength on complex turbidity and saturation binding amount, both of which decreased upon increasing ionic strength. At low ionic strength (1−10 mM), SPB was strongly stretched by the osmotic pressure, which provided enough free volume between the polyelectrolyte chains to accommodate proteins. So the binding amount was large at low ionic strength, which resulted in the enhanced aggregation size and amount. At higher ionic strength (50−500 mM), the added salt led to a screening of the electrostatic interaction between BSA and SPBs, thus the binding amount of BSA by SPB was decreased markedly. At ionic strength of 1000 mM, the electrostatic interaction was almost fully screened, and both the binding amount and turbidity were close to zero. Figure 9b indicates the coincidence between binding amount and turbidity, ensuring the validity of turbidimetric titration technique.

Figure 10 indicates that aggregation and releasing regions can be shifted by changing bulk stoichiometry, which denotes the initial mass concentration ratio of BSA to SPBs. The initial complex aggregation was shifted to low pH, and the maximum turbidity increased with increasing bulk stoichiometry. The pH

Table 3. Binding Parameters of BSA/BLG/Papain−SPB at I = 5 mM

	N	K_{obs} (M^{-1})	ΔH (cal/mol)	ΔS [cal/(mol·K)]
BSA	$(7.9 \pm 0.1) \times 10^3$	$(1.3 \pm 0.2) \times 10^6$	$(-2.7 \pm 0.1) \times 10^4$	−63
BLG	$(1.9 \pm 0.1) \times 10^4$	$(9.6 \pm 4.9) \times 10^6$	$(-2.2 \pm 0.1) \times 10^4$	−41
papain	$(5.7 \pm 0.4) \times 10^3$	$(8.3 \pm 1.9) \times 10^4$	$(-2.4 \pm 0.3) \times 10^3$	14

dx.doi.org/10.1021/bm301865g | Biomacromolecules 2013, 14, 818−827

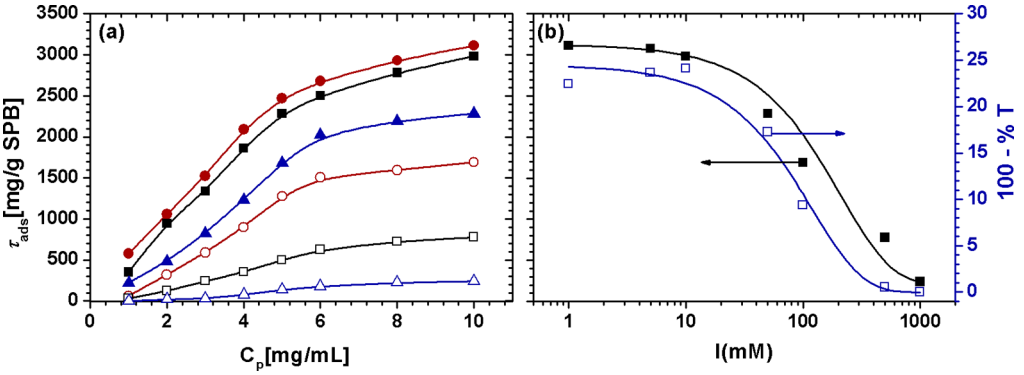

Figure 9. (a) The binding amount of BSA τ_{ads} per unit mass particles is plotted against the original protein concentration in solution C_p. Symbols denote various ionic strength: (●) 1, (■) 10, (▲) 50, (○) 100, (□) 500, and (△) 1000 mM, pH = 6.0. (b) Turbidity (□) and saturation binding amount (■) for BSA−SPB complexes as a function of ionic strength at pH 6.0. BSA and SPB concentrations were 0.020 and 0.004 mg/mL for turbidimetric titration, respectively. Bulk stoichiometry was set as 5 for BSA/SPB (w/w). The cationic SPBs were 75 mol % doses of AEMH monomer.

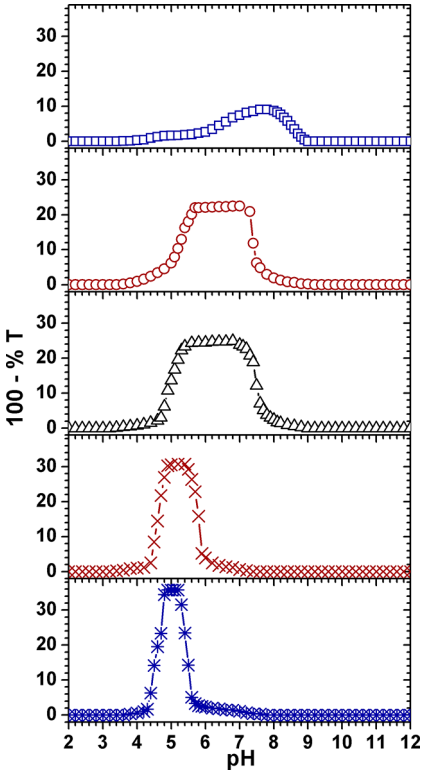

Figure 10. Turbidimetric titration for BSA−SPB as a function of pH at ionic strength of 10 mM in 0.004 mg/mL SPBs (with 75 mol % dose of AEMH) with various BSA concentrations. Symbols denote r = BSA/SPB (w/w) (□) r = 1, (○) r = 3, (△) r = 5, (×) r = 50, and (∗) r = 100.

region of aggregation was narrowed, and releasing occurred at lower pH with increased bulk stoichiometry.

The number of bound protein molecules per SPB chain will increase with increasing the bulk stoichiometry from 1 to 100, which may be attributed to the reduced net charge of SPBs neutralized by more BSA. So the repulsive force among SPBs was reduced, and enhanced aggregation among SPBs could be formed, which led to the increased aggregation size and turbidity. SPBs with less net charge led to a narrower pH range to change net charge and thus to form aggregation. So the onset of releasing shifted to low pH, and the pH region of aggregation was reduced.

On the basis of which has been described above, the different pH regions of aggregation between SPBs and BSA, BLG, and papain can be applied to protein separation and purification (Figure 11). For proteins with various sizes, isoelectric points

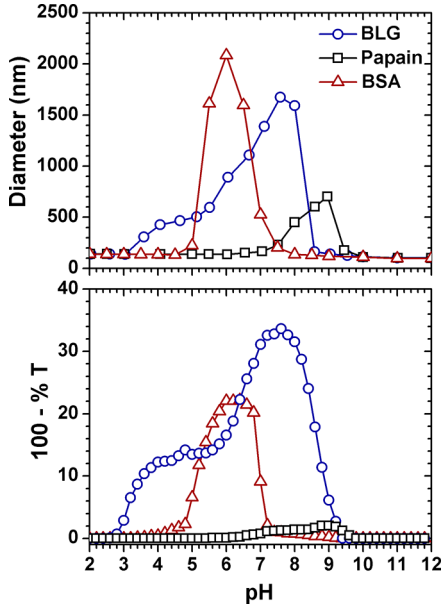

Figure 11. Size and turbidity of complexes between various proteins and cationic SPBs (with 50 mol % dose of AEMH) as a function of pH in 1 mM NaCl solutions under the same conditions. Symbols denote (△) BSA−SPB complexes, (○) BLG−SPB complexes, and (□) papain−SPB complexes. Proteins and SPB concentration are 0.020 and 0.004 mg/mL for turbidimetric titration, and 0.040 and 0.008 mg/mL for DLS, respectively. Bulk stoichiometry was set as 5 for protein/SPB (w/w).

may be separated by cationic SPB. The binding region between protein and cationic SPBs could be controlled by modulating pH and bulk stoichiometry, while the separation efficiency could be tuned by changing the ionic strength. Furthermore, the pH regions of dynamic equilibrium binding can be applied to protein immobilization and enzymatic catalysis.

dx.doi.org/10.1021/bm301865g | *Biomacromolecules* 2013, 14, 818−827

4. CONCLUSIONS

Cationic SPBs synthesized by photoemulsion polymerization were employed as the carriers for the binding of various proteins in aqueous solution. Turbidimetric titration, DLS, and zeta potential were used to investigate the binding event between proteins and cationic SPBs in the full pH window at a certain ionic strength and bulk stoichiometry. The results showed that changing pH could modulate the binding, aggregation, and releasing region. Cationic SPBs bind acidic proteins (BSA/BLG) more strongly than basic protein (papain). The sequence of binding affinity and stoichiometry of proteins onto SPBs was observed by ITC as BLG > BSA > papain, which resulted from the size and charge distribution of proteins. The pH region of binding, aggregation, and releasing between protein and SPBs can also be tuned by modulating bulk stoichiometry. Additionally, the binding amount could be tuned by ionic strength. Therefore, cationic SPBs have potential applications in separation and selective binding of proteins, enzymes, or other biomacromolecules.

AUTHOR INFORMATION

Corresponding Author

*E-mail: guoxuhong@ecust.edu.cn (X.G.); lili76131@ecust.edu.cn (L.L.).

Author Contributions

[§]Siyi Wang and Kaimin Chen contributed equally to this work.

Notes

The authors declare no competing financial interest.

ACKNOWLEDGMENTS

We gratefully acknowledge the National Natural Science Foundation of China (No. 51273063), the Fundamental Research Funds for the Central Universities, the higher school specialized research fund for the doctoral program (20110074110003), and the China Postdoctoral Science Foundation (2012M511088) for support to this work.

REFERENCES

(1) Cooper, C. L.; Dubin, P. L.; Kayitmazer, A. B.; Turksen, S. *Curr. Opin. Colloid Interface Sci.* **2005**, *10*, 52−78.

(2) Turgeon, S. L.; Schmitt, C.; Sanchez, C. *Curr. Opin. Colloid Interface Sci.* **2007**, *12*, 166−178.

(3) Welsch, N.; Becker, A. L.; Dzubiella, J.; Ballauff, M. *Soft Matter* **2012**, *8*, 1428−1436.

(4) Bao, J.; Chen, W.; Liu, T.; Zhu, Y.; Jin, P.; Wang, L.; Liu, J.; Wei, Y.; Li, Y. *ACS Nano* **2007**, *1*, 293−298.

(5) Gu, H.; Xu, K.; Xu, C.; Xu, B. *Chem. Commun.* **2006**, 941−949.

(6) Mahmoudi, M.; Lynch, I.; Ejtehadi, M. R.; Monopoli, M. P.; Bombelli, E. B.; Laurent, S. *Chem. Rev.* **2011**, *111*, 5610−5637.

(7) Haupt, B.; Neumann, Th.; Wittemann, A.; Ballauff, M. *Biomacromolecules* **2005**, *6*, 948−955.

(8) Wittemann, A.; Ballauff, M. *Anal. Chem.* **2004**, *76*, 2813−2819.

(9) Henzler, K.; Wittemann, A.; Breininger, E.; Ballauff, M.; Rosenfeldt, S. *Biomacromolecules* **2007**, *8*, 3674−3681.

(10) Guo, X.; Ballauff, M. *Langmuir* **2000**, *16*, 8719−8726.

(11) Guo, X.; Ballauff, M. *Phys. Rev. E* **2001**, *64*, 051406.

(12) Ballauff, M.; Borisov, O. *Curr. Opin. Colloid Interface Sci.* **2006**, *11*, 316−323.

(13) Ballauff, M. *Prog. Polym. Sci.* **2007**, *32*, 1135−1151.

(14) Czeslik, C. *Z. Phys. Chem.* **2004**, *218*, 771−801.

(15) Czeslik, C.; Winter, R. *Phys. Chem. Chem. Phys.* **2001**, *3*, 235−239.

(16) Czeslik, C.; Jackler, G.; Hazlett, T.; Gratton, E.; Steitz, R.; Wittemann, A.; Ballauff, M. *Phys. Chem. Chem. Phys.* **2004**, *6*, 5557−5563.

(17) Chen, K.; Zhu, Y.; Li, L.; Lu, Y.; Guo, X. *Macromol. Rapid Commun.* **2010**, *31*, 1440−1443.

(18) Chen, K.; Zhu, Y.; Zhang, Y.; Li, L.; Lu, Y.; Guo, X. *Macromolecules* **2011**, *44*, 632−639.

(19) Wu, S.; Kaiser, J.; Guo, X.; Li, L.; Lu, Y.; Ballauff, M. *Ind. Eng. Chem. Res.* **2012**, *51*, 5608−5614.

(20) Welsch, N.; Wittemann, A. *J. Phys. Chem. B* **2009**, *113*, 16039−16045.

(21) Lu, Y.; Proch, S.; Schrinner, M.; Drechsler, M.; Kempe, R.; Ballauff, M. *J. Mater. Chem.* **2009**, *19*, 3955−3961.

(22) Anikin, K.; Rocker, C.; Wittemann, A.; Wiedenmann, J.; Ballauff, M.; Nienhaus, G. U. *J. Phys. Chem. B* **2005**, *109*, 5418−5420.

(23) Rosenfeldt, S.; Wittemann, A.; Ballauff, M.; Breininger, E.; Bolze, J.; Dingenouts, N. *Phys. Rev. E* **2004**, *70*, 061403−061413.

(24) Xia, J.; Dubin, P. L.; Dautzenberg, H. *Langmuir* **1993**, *9*, 2015−2019.

(25) Kayitmazer, A. B.; Strand, S. P.; Tribet, C.; Jaeger, W.; Dubin, P. L. *Biomacromolecules* **2007**, *8*, 3568−3577.

(26) Antonov, M.; Mazzawi, M.; Dubin, P. L. *Biomacromolecules* **2010**, *11*, 51−59.

(27) Mattison, K. W.; Dubin, P. L.; Brittain, I. J. *J. Phys. Chem. B* **1998**, *102*, 3830−3836.

(28) Mattison, K. W.; Brittain, I. J.; Dubin, P. L. *Biotechnol. Prog.* **1995**, *11*, 632−637.

(29) Becker, A. L.; Welsch, N.; Schneider, C.; Ballauff, M. *Biomacromolecules* **2011**, *12*, 3936−3944.

(30) Wittemann, A.; Ballauff, M. *Macromol. Biosci.* **2005**, *5*, 13−20.

(31) De, M.; Miranda, O. R.; Rana, S.; Rotello, V. M. *Chem. Commun.* **2009**, 2157−2159.

(32) Schrinner, M.; Proch, S.; Mei, Y.; Kempe, R.; Miyajima, N.; Ballauff, M. *Adv. Mater.* **2008**, *20*, 1928−1933.

(33) Schrinner, M.; Ballauff, M.; Talmon, Y.; Kauffmann, Y.; Thun, J.; Moller, M.; Breu, J. *Science* **2009**, *323*, 617−620.

(34) Sharma, G.; Ballauff, M. *Macromol. Rapid Commun.* **2004**, *25*, 547−552.

(35) Guo, X.; Weiss, A.; Ballauff, M. *Macromolecules* **1999**, *32*, 6043−6046.

(36) Mei, Y.; Wittemann, A.; Sharma, G.; Ballauff, M.; Koch, Th.; Gliemann, H.; Horbach, J.; Schimmel, Th. *Macromolecules* **2003**, *36*, 3452−3456.

(37) Mei, Y.; Ballauff, M. *Eur. Phys. J. E* **2005**, *16*, 341−349.

(38) Wittemann, A.; Ballauff, M. *Phys. Chem. Chem. Phys.* **2006**, *8*, 5269−5275.

(39) Wittemann, A.; Ballauff, M. *Phys. Chem. Chem. Phys.* **2003**, *5*, 1671−1677.

(40) Volk, N.; Vollmer, D.; Schmidt, M.; Oppermann, W.; Huber, K. *Adv. Polym. Sci.* **2004**, *166*, 29−65.

(41) Kayitmazer, A. B.; Quinn, B.; Kimura, K.; Ryan, G. L.; Tate, A. J.; Pink, D. A.; Dubin, P. L. *Biomacromolecules* **2010**, *11*, 3325−3331.

(42) Silva, R. A.; Urzua, M. D.; Petri, D. F. S.; Dubin, P. L. *Langmuir* **2010**, *26*, 14032−14038.

(43) Seyrek, E.; Dubin, P. L.; Tribet, C.; Gamble, E. A. *Biomacromolecules* **2003**, *4*, 273−282.

(44) Biesheuvel, P. M.; Wittemann, A. *J. Phys. Chem. B* **2005**, *109*, 4209−4214.

(45) Biesheuvel, P. M.; Leermakers, F. A. M.; Stuart, M. A. C. *Phys. Rev. E* **2006**, *73*, 011802−011811.

(46) Leermakers, F. A. M.; Ballauff, M.; Borisov, O. V. *Langmuir* **2007**, *23*, 3937−3946.

(47) de Vos, W. M.; Leermakers, F. A. M.; de Keizer, A.; Stuart, M. A. C.; Kleijn, J. M. *Langmuir* **2010**, *26*, 249−259.

(48) de Vos, W. M.; Biesheuvel, P. M.; de Keizer, A.; Kleijn, J. M.; Stuart, M. A. C. *Langmuir* **2008**, *24*, 6575−6584.

(49) Wittemann, A.; Haupt, B.; Ballauff, M. *Z. Phys. Chem.* **2007**, *221*, 113−126.

(50) da Silva, F. L. B.; Lund, M.; Jonsson, B.; Akesson, T. *J. Phys. Chem. B* **2006**, *110*, 4459−4464.
(51) De, M.; You, C. C.; Srivastava, S.; Rotello, V. M. *J. Am. Chem. Soc.* **2007**, *129*, 10747−10753.
(52) Xu, Y.; Mazzawi, M.; Chen, K.; Sun, L.; Dubin, P. L. *Biomacromolecules* **2011**, *12*, 1512−1522.
(53) Chen, K.; Xu, Y.; Rana, S.; Miranda, O. R.; Dubin, P. L.; Rotello, V. M.; Sun, L.; Guo, X. *Biomacromolecules* **2011**, *12*, 2552−2561.
(54) Henzler, K.; Haupt, B.; Lauterbach, K.; Wittemann, A.; Borisov, O.; Ballauff, M. *J. Am. Chem. Soc.* **2010**, *132*, 3159−3163.